Appl Biochem Biotechnol (2010) 160:1888–1895
DOI 10.1007/s12010-009-8726-5

Nickel-Impregnated Silica Nanoparticle Synthesis and Their Evaluation for Biocatalyst Immobilization

Reddy Shetty Prakasham · G. Sarala Devi · Chaganti Subba Rao · V. S. S. Sivakumar · T. Sathish · P. N. Sarma

Received: 24 September 2008 / Accepted: 26 July 2009 /
Published online: 16 August 2009

Abstract In the present investigation, impact of nickel-impregnated silica paramagnetic particles (NSP) as biocatalyst immobilization matrices was investigated. These nanoparticles were synthesized by sol–gel route using a nonionic surfactant block co polymer [poly (ethylene glycol)-*block*-poly-(propylene glycol)-*block*-poly (ethylene glycol)]. Diastase enzyme was immobilized on these particles (enzyme-impregnated NSP) as model enzyme and characterized using Fourier-transform infrared spectroscopy and X-ray crystallography. Analysis of enzyme-binding nature with these nanoparticles at different physiological conditions revealed that binding pattern and activity profile varied with the pH of the reaction mixture. The immobilized enzyme was further characterized for its biocatalytic activity with respect to kinetic properties such as Km and Vmax and compared with free enzyme. Paramagnetic nanoparticle-immobilized enzyme showed more affinity for substrate compared to free one. The nature of silica and nickel varied from amorphous to crystalline nature and vice versa upon immobilization of enzyme. To the best of our knowledge, this is the first report of its kind for change of nature from one form to other under normal temperatures upon diastase interaction with NSP.

Keywords Diastase · Nickel–silica nanoparticles · Immobilization/impregnation · Enzyme kinetics

R. S. Prakasham (✉) · G. S. Devi (✉) · C. S. Rao · T. Sathish · P. N. Sarma
Bioengineering and Environmental Centre, Indian Institute of Chemical Technology,
Hyderabad 500007, India
e-mail: prakasam@iict.res.in
e-mail: sarala@iict.res.in

G. S. Devi · V. S. S. Sivakumar
Inorganic and Physical Chemistry Division, Indian Institute of Chemical Technology,
Hyderabad 500007, India

Introduction

In the present ecofriendly-driven world, nanotechnology is revolutionizing the modern biotechnology mainly due to nanoparticle-exemplified specific properties due to interdisciplinary areas playing vital role in various technological developmental sectors. Among all, biosystems and its components have remarkable impact as biotechnology deals with nanometer size molecules such as protein and nucleic acids. In fact, the combination of biotechnology and semiconductor technology is emerging as a promising candidate for enabling a breakthrough in the fabrication of advanced electronic devices [1, 2]. Several bio-nano processes (BNP) were developed using fabricated nanoscale structures with biomolecules as nanoblocks [3]. In all these BNPs, the interactive nature between the biological component and nanomaterial play an important role on alteration of components properties and their subsequent usage. In fact, the knowledge of the morphology and the structure of the alloys is a crucial point for biomolecule attachment, its super elastic properties, shape-based memory, and associated regulation of functional behavior of the biocatalyst [4]. Though conventional interaction technology has been extensively studied for its application potential using either whole-cell microbial systems or isolated biocatalysts at different industrial as well as other pharma-related sectors, it was generally noticed that all these methodologies related with non-biocomponent which alters the properties of the interacted bioelement [5]. Recently, aerosol methods have been developed to produce nanostructured materials in which sols of silica and titania nanoparticles are sprayed and dried during the flight of the sol droplets [6, 7]. Ohshima et al. [8] prepared spray-pyrolyzed precursors by dissolving zinc salt in TiO_2 sol to prepare ZnO–titania aggregate particles. The salt concentration and temperature were major variables used in this study with silica sol concentration kept constant. Conventional liquid-phase preparation methods for such particles have had inherent limitations on satisfying the demands. However, a few reports are available on impregnation of enzymes on nickel–silica particles.

Nickel nanoparticles dispersed in porous silica structures have been long used as catalysts for hydrogenation, hydrogenolysis, reforming, gas shift reaction, etc. [9–11] in addition to its potential applications in a variety of optical, nanoelectronic, and optoelectronic devices [12]. They have been mainly prepared either by direct impregnation of nickel salt or deposition–precipitation of nickel oxide from the nickel salt into the pores of silica followed by reduction with hydrogen. The sol–gel technology is presently believed to be one of the most promising approaches for the attachment of enzymes due to its entrapment process occurring without formation of covalent linkages between biomolecules and matrix leaving the enzymes in their intact state. Generally, sol–gel derived materials are fabricated on the base of oxides of various metals like alumina, titania, and zirconia. The entrapment of enzymes is usually performed by using silica because of its better biocompatibility. Though iron–silica composites have been studied for enzyme immobilization, however, little reports are available in literature on use of nickel–silica nanoparticles as enzyme immobilization matrices. Keeping this in view, silica–nickel composite was synthesized by sol–gel method. A model enzyme, amylase, was used in this study, and its adsorption behavior on these particles was characterized by Fourier-transform infrared (FTIR), X-ray diffraction studies (XRD), and energy dispersive X-ray (EDX). The impregnated enzyme on silica–nickel particles was characterized for its biocatalytic behavior under different temperature and pH environments in addition to its kinetic properties and compared with free enzyme activities.

Materials and Methods

Preparation of the Nickel-Impregnated Silica Nanoparticles

Sol–gel process was adopted for synthesis of nickel-impregnated silica nanoparticles (NSP). The synthesized material was characterized by X-ray diffraction studies to confirm the formation of crystal phase. Further, elemental analysis and purity of the synthesized sample was analyzed by EDX technique.

Preparation of Enzyme-Impregnated NSP

Commercially available amylase enzyme (Sigma-Aldrich, USA) was used in this investigation. A 100-mg amount of enzyme was dissolved in 1 mL of distilled water, and to this, 100 mg of synthesized matrix particles was added under nitrogen atmosphere. This mixture was incubated at 30°C for 30 min under constant mixing environment. The contents were then centrifuged at 10,000 rpm for 5 min at 30°C. The unbound enzyme from these particles was removed by washing with sterilized distilled water until the supernatant was free of protein and/or enzyme activity. These enzyme-impregnated NSP (EI-NSP) were dried using a vacuum evaporator and used for characterization and evaluation of its biological activity.

Characterization of NSP and EI-NSP

NSP and EI-NSP were characterized for their surface chemistry and morphology to understand the nature of physicochemical properties and enzyme binding using different analytical techniques (XRD and FTIR, etc.). X-ray Diffraction (XRD D/8 BRUKER AXS operating at 40 kV at a current of 30 mA with Cu Kα radiation) was used to identify the composites and observe their crystallinity by continuous scan from 0° to 80° before and after enzyme-bound NSP. Chemical bonds in the composites were identified with Fourier-transform infrared spectroscopy (Thermo Nicolet Nexus 670spectrometer). Demoisturized samples before and after enzyme binding (1–2 mg) were homogenized with 100 mg of dry KBr and made into pellets. These pellets were analyzed for transmittance in the range of 4,000 to 400 cm^{-1}.

Enzyme Activity Measurement

The enzyme activity was measured according to [16] by estimating the maltose produced during starch hydrolysis using 3,5-dinitrosalicylic acid as a coupling reagent. The reaction mixture containing 1.0 mL of 1% soluble starch in 0.01 M phosphate buffer (pH5.0) and 10 mg of EI-NSP was incubated at 30°C for 5 min and centrifuged to separate the EI-NSP and the reaction mixture. The reaction was stopped by adding 2.0 mL of 3,5-dinitrosalicylic acid solution followed by heating in a boiling water bath for 5 min. The contents were then cooled to room temperature, and the volume was made up to 10 mL with distilled water. The absorbance of the reaction mixture was determined at 540 nm in a UV–visible spectrophotometer. The temperature effect on the enzyme was studied by performing the reaction at predetermined temperature. One unit of the enzyme was defined as the amount of enzyme capable of producing 1 M reducing sugar (as maltose) from 1% soluble starch as substrate in 1 min at 30°C.

Calculation of Km, Vmax, Activation Energy Values, and Protein Estimation

Reaction kinetics for EI-NSP and free enzyme were estimated by measuring the catalytic activity at different substrate concentrations. Km and Vmax values were calculated by representing the enzyme activity values at different substrate concentrations in a Lineweaver–Burk equation. The protein content of the enzyme was estimated according to the method of Lowry et al [13].

Results and Discussion

Synthesis of NSP

In a typical procedure, tetra ethyl ortho silicate (TEOS) was used for synthesis of NSP as raw silica source. TEOS (0.016 mol) was dissolved slowly in acidified co-block polymer solution under constant mixing environment to get uniform solution to promote hydration of TEOS and decrease of residual ethoxy groups affecting the assembly of the particles. Subsequently, $NiSO_4$ in 1:4 molar ratio of silica to nickel was added and stirred for 24 h. The resulting reactant was neutralized with 25% ammonia solution to get effective formation of ordered nanoparticles through self-assembly of silicate and nonionic co-block polymer as influenced by the decrease in polarity with the assembly of the species. Co-block polymer nonionic surfactant surrounded the silica composite and thus acted as a grain growth inhibitor and stabilized the ordered nanoparticles. Finally, the solution was aged for 24 h at room temperature, centrifuged, washed with de-ionized water, rinsed with distilled acetone, and oven dried in order to get silica-impregnated nickel nanoparticles (NSP), which were further calcined at 500 °C under N_2 atmosphere.

Enzyme-Binding Studies

The diastase enzyme-binding pattern with respect to solution pH was investigated by using a 1:1 ratio of NSP and enzyme (*w*/*w*). After thorough mixing for 30 min at room temperature, the contents were centrifuged to remove the unbound enzyme present in the solution. The enzyme concentration in the supernatant was determined in terms of protein content, and the immobilized enzyme was calculated by deducting the enzyme present in the solution before binding studies.

Characterization of NSP and EI-NSP

The purity of NSP thus synthesized was confirmed by EDX analysis. The results revealed that the only detected elements present in these nanoparticles were Si, Ni, and O with 39.70%, 5.14%, and 54.70%, respectively. No other impurities in the prepared silica–nickel particles were detected. This confirms the purity of the synthesized sample.

Further analysis of the prepared NSP and EI-NSP were characterized using X-ray diffraction. Figure 1a shows the powder X-ray diffractograms of NSP. Broad peaks observed at $2\theta = 19°$, 22°, and 28° were attributed to SiO_2. The diffractogram did not show any peaks corresponding to NiO, which were generally reflected at 63°. This may be due to the fact that the nickel oxide particles in the samples may be amorphous in nature or more likely too small (below 3 nm) to give a XRD pattern (Fig. 1a). However,

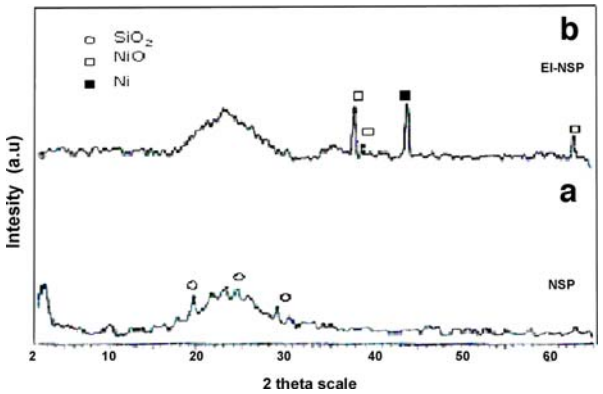

Fig. 1 XRD pattern of NSP and EI-NSP

the peak intensities of nickel oxide were noticed after enzyme immobilization on NSP (Fig. 1b) indicating its crystalline nature upon enzyme immobilization. Thus, the nature of nickel on the NSP was getting modified during interaction with enzyme as these peaks were noticed only with EI-NSP and not with NSP (Fig. 1). Apart from nickel oxide, a peak corresponding to metallic Ni was also observed at $2\theta=43°$. No peaks were noticed for SiO_2 presence in EI-NSP, suggesting that upon enzyme binding, silica may be losing its crystalline nature. However, increase in NiO peak intensity at 38° and 39° suggest an indirect evidence for enzyme incorporation-associated change in silica and nickel in these particles. To the best of our knowledge, this is the first report on change of silica and nickel particles from crystalline to amorphous and vice versa before and after immobilization, respectively. However, the variation of silica nature from amorphous to crystalline was observed in nickel-containing silica products [14].

Figure 2 shows FTIR spectra of the composites of NSP and EI-NSP. The characteristic peaks of Si–O–Si asymmetric bending were observed at 1,087 and 798 cm^{-1}. However, a slight shift to lower values of 1,032 and 789 cm^{-1} were noticed with EI-NSP sample

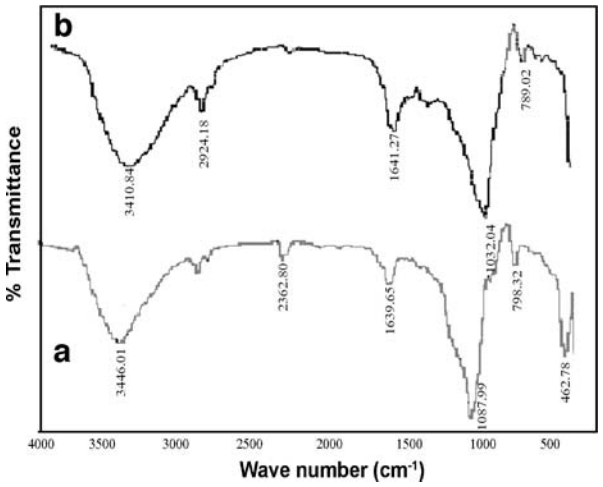

Fig. 2 FTIR spectra of NSP (**a**) and EI-NSP (**b**)

(Fig. 2b). The peak at 1,639 cm^{-1} corresponds to H–O–H bending, while the peak observed at 2,362 cm^{-1} was probably related with the formation of the nickel oxide compound. The presence of the peak at 2,924 cm^{-1} in the EI-NSP does suggest methylene antisymmetric and symmetric vibrations, which may be due to presence of enzyme. This was further evidenced from an intense OH stretching band in the range of 3,410–3,446 cm^{-1} after enzyme binding, depicting the presence of enzyme on the surface of the particles.

Biocatalytic Evaluation of EI-NSP

The effect of pH on the enzyme activity (free and impregnated) was investigated in the range of pH3–7, and results were shown in Fig. 3. It was observed that enzyme activity varied with the solution pH and maximum activity noticed at pH5.0 in both free and impregnated environments. In all studied environments, EI-NSP revealed more catalytic behavior (approximately 40%) compared to its counterpart, indicating that immobilization of enzyme on these NSP protects its deactivation by solution pH. In addition, the improved enzyme activity may be attributed to the fact that configuration of enzyme was altered under immobilized environment. Such variation of improved activity under immobilized conditions was observed with other microbial systems and enzymes [5, 15, 16].

Further, the diastase enzyme immobilized on NSP was evaluated for starch hydrolysis function at different incubation temperature conditions ranging from 303 to 333 K at pH5.0. NSP-immobilized enzyme showed improved starch hydrolysis activity compared to free enzyme in all studied incubation temperatures suggesting enhanced thermostability upon immobilization on to NSP (Fig. 4). These results were in accordance with the data where enhanced biocatalytic activity was observed under immobilized conditions with various matrices [5, 16]. Incubation temperature dependent catalytic activity for both (free and immobilized) enzymes was also noticed. However, variation of activity profile differed with incubation temperature (Fig. 4). Only slight variation in enzyme activity was observed with the variation of reaction mixture temperature from 303 to 313 K, and further increase resulted in drastic reduction of biocatalytic activity. The maximum activity was observed at 313 K. Therefore, immobilized enzyme kinetics was investigated at 313 K and compared with free enzyme.

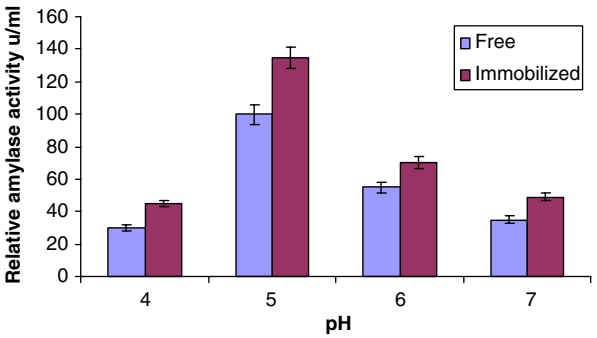

Fig. 3 Influence of pH on free and immobilized enzyme activity

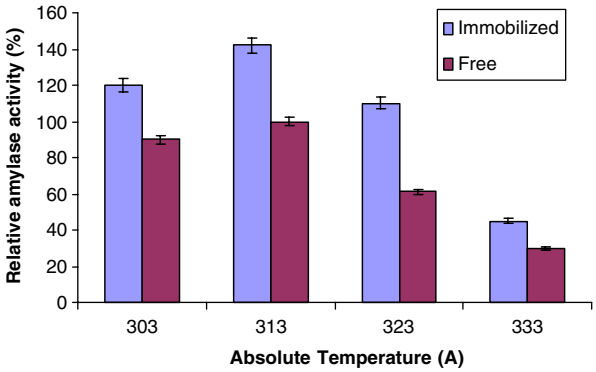

Fig. 4 Effect of incubation temperature on the biocatalytic activity of free and immobilized enzyme

The Km value for an enzymatic reaction determines the affinity of the enzyme for the substrate, whereas the value of Vmax provides the maximum rate of enzyme reaction when the enzyme was saturated by the substrate. The smaller value of Km indicates the increased affinity of enzyme for substrate. Substrate-dependent amylase activity increased with the increase in starch concentration up to 8 μM, and further increase did not show much variation. Values of kinetic parameter (Km and Vmax) were determined by the analysis of the slope of enzymatic reactions using the Lineweaver–Burk plot. Km values in the present enzymatic assay were found to be 8,414 and 10,176 mM for the immobilized and free amylase, respectively. Vmax (4.92 μM $min^{-1} mg^{-1}$) obtained for the immobilized amylase was one order higher in magnitude than that of free amylase (2.71 μM $min^{-1} mg^{-1}$). However, the value of Km for the immobilized amylase was 1.81-fold lower in magnitude in comparison with the value obtained for free amylase, indicating its efficiency under immobilized environment. To clarify further that the reaction rates observed with the immobilized enzyme are not associated with enzyme molecules released from the particles, all experiments were repeated after removal of immobilized enzyme nanoparticles from the reaction medium, using final reaction mixture as control. The data revealed little increase in enzyme activity, indicating that the substrate conversion is associated with immobilized enzyme only, and no enzyme is released during catalysis reaction.

Conclusions

In the present investigation, nickel–silica nanoparticles (NSP) were synthesized by sol–gel route using nonionic surfactant (co-block polymer). XRD studies confirm that the synthesized NSP contain SiO_2. The change from amorphous to crystalline nature in case of nickel and vice versa with silica upon enzyme immobilization on NSP was observed, and this is the first report of such kind at normal temperature. These nanoparticles were used as a matrix for enzyme diastase immobilization. Confirmation of the enzyme binding was demonstrated by FTIR and XRD studies. Enzyme binding at different pH environments revealed that enzyme loading differs with the pH of the reaction medium. Higher enzyme loading was observed at pH5. Kinetic data indicated that the catalysis occurs at lower activation energy levels with immobilized enzyme compared to free enzyme.

Acknowledgment The authors thank the Department of Science and Technology, New Delhi, for financial support. Ch Subba Rao and T Sathish are thankful to CSIR and APNL for financial support in the form of fellowship.

References

1. Hikono, T., Uraoka, Y., Fuyuki, T., & Yamashita, I. (2003). *Japanese Journal of Applied Physics, 42*, 398–399. doi:10.1143/JJAP.42.L398.
2. Yoshii, S., Yamada, K., Matsukawa, N., & Yamashita, I. (2005). *Japanese Journal of Applied Physics, 44*, 1518–1523. doi:10.1143/JJAP.44.1518.
3. Yamashita, I. (2001). *Thin Solid Films, 393*, 12–18. doi:10.1016/S0040-6090(01)01083-5.
4. Duerig, W., Pelton, A. R., & Stöckel, D. (1997). *Med Plast & Biomater Magazine*, United States Patent 7128757, 1–14.
5. Ramkrishna, S. V., & Prakasham, R. S. (1999). *Current Science, 77*, 87–100.
6. Kim, J., Wilhelm, O., & Pratsinis, S. E. (2001). *Journal of the American Ceramic Society, 84*, 2802–2808.
7. Iskandar, F., Gradon, L., & Okuyama, K. (2003). *Journal of Colloid and Interface Science, 265*, 296–303. doi:10.1016/S0021-9797(03)00519-8.
8. Ohshima, K., Tsuto, K., Okuyama, K., & Tohge, N. (1993). *Aerosol Science and Technology, 19*, 468–477. doi:10.1080/02786829308959652.
9. Gonzalez-Marcos, M. P., Gutirrez-Ortiz, J. I., de Elguea, C. G.-O., Delgado, J. A., & Gonzalez-Velasco, J. R. (1997). *Applied Catalysis. A., General, 162*, 269–280. doi:10.1016/S0926-860X(97)00111-7.
10. Ueckert, T., Lamber, R., Jaeger, N. I., & Schubert, U. (1997). *Applied Catalysis. A, General, 155*, 75–85. doi:10.1016/S0926-860X(96)00384-5.
11. Ermakova, M. A., Ermakov, D. Y., Cherepanova, S. V., & Plyasova, L. M. (2002). *The Journal of Physical Chemistry B, 106*, 11922–11928. doi:10.1021/jp021231q.
12. De, G., Licciulli, A., Massaro, C., Tapfer, L., Catalano, M., Battaglin, G., et al. (1996). *Journal of Non-Crystalline Solids, 194*, 225–234. doi:10.1016/0022-3093(91)00511-F.
13. Lowry, O. H., Rosebrough, N. J., Farr, A. L., & Randall, R. J. (1951). *Journal of Biological Chemistry, 193*, 265–275.
14. Kim, H. S., Kim, C. S., & Kim, S. G. (2006). *Journal of Non-Crystalline Solids, 352*, 2204–2212. doi:10.1016/j.jnoncrysol.2006.02.040.
15. Srinivasulu, B., Prakasham, R. S., Annapurna, J., Srinivas, S., Ellaiah, P., & Ramakrishna, S. V. (2002). *Process Biochemistry, 38*, 593–598. doi:10.1016/S0032-9592(02)00182-6.
16. Prakasham, R. S., Sarala Devi, G., Rajya Laxmi, K., & Subba Rao, Ch. (2007). *Journal of Physics and Chemistry. C, 111*, 3842–3847. doi:10.1021/jp0670182.